Extreme Mechanics Letters 41 (2020) 101045

Contents lists available at ScienceDirect

Extreme Mechanics Letters

journal homepage: www.elsevier.com/locate/eml

Oxidation weakens interfaces in carbon nanotube reinforced titanium nanocomposites: An *in situ* electron microscopy nanomechanical study

Christopher M. Dmuchowski [a,b,1], Chenglin Yi [a,1], Feilin Gou [a], Anju Sharma [c], Cheol Park [d], Changhong Ke [a,b,*]

[a] Department of Mechanical Engineering, State University of New York at Binghamton, Binghamton, NY 13902, USA
[b] Materials Science and Engineering Program, State University of New York at Binghamton, Binghamton, NY 13902, USA
[c] Small Scale Systems Integration and Packaging Center, State University of New York at Binghamton, Binghamton, NY 13902, USA
[d] Advanced Materials and Processing Branch, NASA Langley Research Center, Hampton, VA 23681, USA

ARTICLE INFO

Article history:
Received 14 May 2020
Received in revised form 4 September 2020
Accepted 26 September 2020
Available online 16 October 2020

Keywords:
Interfacial strength
Carbon nanotubes
Titanium
Metal matrix nanocomposites
Oxidation

ABSTRACT

The interfacial binding interactions in fiber–reinforced metal matrix nanocomposites (MMNC) are involved with sophisticated physico-chemical phenomena that are sensitive to their commonly encountered high-temperature processing and/or working environments. The resulting interfacial load transfer characteristics, which play a vital role in achieving the anticipated bulk mechanical properties enhancements, remain elusive. Here we investigate the effect of thermal processing on the interfacial strength of carbon nanotube (CNT) reinforced titanium (Ti) nanocomposites by conducting *in situ* nanomechanical single-nanotube pull-out measurements inside a high resolution scanning electron microscope. Our nanomechanical measurements reveal that thermal annealing at 400 °C for two hours results in a 40% decrease of the interfacial load-carrying capacity. The measurements were analyzed using a micromechanics shear-lag model, and the results show that the thermal annealing reduces the maximum interfacial shear strength by about 42% from about 231MPa to about 135 MPa. The observed weakening of the CNT–Ti interface caused by thermal annealing is attributed to the formation of newly grown titanium oxide on the CNT–Ti binding interface. The findings reported here are useful to better understand the impact of thermal processing on the reinforcing efficiency of nanotubes in metal matrices, which is essential to the design and manufacturing of nanotube-reinforced MMNC with superior high-temperature performance.

1. Introduction

The envisioned light, strong, durable, and thermally/chemically stable properties of nanofiber–reinforced metal matrix nanocomposites (MMNC) are attractive to a number of industries, such as the aerospace, automotive, chemical and biomedical industries [1–3]. Many of these remarkable property enhancements originate from the superior physical/chemical properties of the added reinforcing nanofibers, such as one-dimensional carbon and boron nitride nanotubes and two-dimensional graphene and hexagonal boron nitride nanosheets [4–6]. Full utilization of these nanofibers' extraordinary material characteristics crucially counts on an efficient load transfer on the fiber–metal interface [3]. The interfacial binding interactions in fiber–reinforced MMNC are involved with sophisticated physico-chemical phenomena that are sensitive to the commonly encountered high-temperature processing and/or working environments. For example, metal oxides may grow on the fiber–metal interface through oxidation reactions. Chemical compounds may also form through the chemical reaction of the added reinforcing fibers with the surrounding metal matrices. The newly formed reaction products may significantly alter the nature of the interfacial binding interactions [7] and the local structural morphology of the contacting interface, the latter of which can further result in changes of contact areas and the local stress state due to processing-induced residual stress and interlocking effects [8]. Therefore, thermal annealing-produced reaction products could have a significant impact on the interfacial load transfer characteristics, which play a vital role in achieving the enhancement of bulk mechanical properties.

Recent experimental studies on the interfacial binding interaction on carbon nanotube (CNT) reinforced aluminum (Al) MMNC shows that oxidation from thermal annealing results in a 40% increase of the interfacial strength [9]. The substantial interfacial strength enhancement was revealed later by density functional theory (DFT) calculations [10], which show that the

* Corresponding author at: Department of Mechanical Engineering, State University of New York at Binghamton, Binghamton, NY 13902, USA.
E-mail address: cke@binghamton.edu (C. Ke).

[1] These two authors contributed equally to this work.

https://doi.org/10.1016/j.eml.2020.101045
2352-4316/

newly formed ionic bonding between Al and O atoms results in a high degree of localization of electron packets near the carbon lattice surface. The resulting cross-interface bonding interaction leads to a significantly stronger interfacial binding interaction as compared with pure CNT–Al binding interaction that is involved with a sharp transition from metallic bonding in metals to covalent bonding in CNTs and lacks any prominent cross-interface bonding. It is worth mentioning that reaction products formed on the fiber–metal interface pose an additional degree of complexity in understanding the interfacial physico-chemical interactions and even the same type of reaction products may influence the interfacial interaction differently across different fiber–metal systems. Therefore, it is essential to investigate the impact of the reaction products produced from thermal processing on the interfacial load transfer characteristics of each type of fiber–reinforced MMNC. Similar to Al, titanium (Ti) is a type of widely used metal matrix materials for MMNC due to its lightweight and high-strength properties and superior corrosion resistance characteristics [11,12]. Several experimental studies report substantial enhancements of the bulk mechanical properties of CNT-reinforced Ti MMNC [13–16]. Specifically, a small fraction of CNT additions to Ti (0.35–0.4%) reportedly increases the yield strength by 40%–48% [13,15] and the compressive strength by 61.5% [14]. These superior bulk property enhancements indicate a qualitatively strong interfacial binding affinity between Ti and CNT. Recently, our research group conducted a quantitative investigation of the mechanical strength of CNT–Ti interfaces through *in situ* single-nanotube pull-out experiments inside a scanning electron microscope (SEM) [10]. The nanomechanical measurements reveal a strong CNT–Ti binding interface, which agrees well with theoretical findings of strong binding affinity of Ti with hexagonal covalent C–C bonding lattices like those in CNTs and graphene [7,17]. Despite these scientific advances, quantitative and microscopic experimental investigation of the influence of thermal processing on the CNT–Ti interface remains unexplored. It is noted that Kondoh et al. reported a decreasing tendency of the bulk mechanical properties of CNT–Ti composite materials at elevated temperatures [18]. The usefulness of such macroscopic measurements in understanding how thermal processing affects the interfacial binding interactions on the CNT–metal interface is limited because the observed degradation of bulk mechanical properties can be attributed to several sources, such as changes of microstructure and properties of metal matrix materials [16,19,20]. In this paper, we tend to address this knowledge gap by quantifying the mechanical strength of CNT–Ti interfaces that are subjected to thermal processing and provide insights on how thermal oxidation affects CNT–Ti binding interactions and the related interfacial load transfer characteristics.

2. Results and discussion

2.1. In situ SEM nanomechanical single-nanotube pull-out measurements of thermally annealed CNT–Ti interfaces

(a) *Testing scheme* Fig. 1(a) illustrates the interfacial strength testing scheme by using an *in situ* SEM nanomechanical single-nanotube pull-out technique, which has been demonstrated in our prior nanomechanical studies of binding interfaces formed by nanotubes with polymers [21–23], metals [9,10] and ceramics [24]. In brief, a straight cantilevered nanotube that is partially embedded in a metal matrix is stretched out by applying a gradually increasing stretching force through displacing an atomic force microscopy (AFM) cantilever. The AFM cantilever, which works as a force sensor, is mounted to a 3D piezo-driven manipulator with ∼1 nm displacement resolution in XYZ axes. The high-resolution electron beam of an FEI Nanolab 600 microscope is used to monitor the displacement of the AFM cantilever and the deformational/failure behaviors of the nanotube during the stretching process and to measure the embedded length of the nanotube once it is fully pulled out of the matrix with a few nanometers in spatial resolution. By using AFM cantilevers (CSG01 from NT-MDT) with thermally calibrated spring constants of 0.04–0.09 N/m, the force measurement resolution of our nanomechanical experimental setup is estimated to be ∼0.5 nN.

(b) *Sample preparation and characterization* The tested CNT–Ti interfaces were engineered inside sandwiched metal/nanotube/metal thin-film composites, which were manufactured by following the protocols reported in our prior work [9,10]. In brief, double-walled carbon nanotubes (DWCNTs), which were produced using chemical vapor deposition methods (purchased from Sigma-Aldrich), were first sonicated in deionized (DI) water with the aid of ionic surfactants for two hours to form well-dispersed nanotube solutions. Our prior AFM measurements [23] show that the employed DWCNTs have a polydispersed diameter between 2.0–4.2 nm with a median diameter of 3.1 nm. A majority of the dispersed nanotubes have lengths shorter than 2 μm and are capable of staying straight after being deposited on flat substrates using spin coating. The sandwiched Ti/CNT/Ti composite was manufactured by depositing the first 100 nm-thick Ti metal film on fresh silicon substrates by using electron beam evaporation, which was conducted inside an ATC Orion 8-E evaporator system (AJA International Inc.) with a Titanium target of 99.999% in purity (Kamis Inc.), a vacuum pressure of 1×10^{-8} Torr and an electron gun accelerating voltage of 7 kV. Subsequently, a well-dispersed CNT solution was deposited on the surface of the deposited Ti film by spin coating in air and then air-dried, followed by the electron beam evaporation of the second 100 nm-thick Ti film. The sandwiched composite specimens were then thermally annealed on a hot plate in air from room temperature to 400 °C at a rate of 2 °C per minute, and then steadily maintained for two hours. After the cool-down of the specimens to room temperature, a diamond scriber was used to fracture the sandwiched composite and some embedded CNTs were protruded from the fracture surfaces as protruding cantilevered structures.

The structural morphology of the electron beam evaporated Ti films with deposited CNTs on top was characterized by using tapping-mode AFM before and after thermal annealing, which is exemplified by the AFM images in Fig. 1(b). The AFM measurements were conducted inside an NTEGRA AFM (NT-MDT) using silicon probes with a nominal tip radius of ∼6 nm. The AFM images clearly show that nanotubes of a few hundred nm in length stay straight after the spin-coating deposition on Ti surfaces that are formed by densely packed Ti grains and are capable of preserving their straight conformations after thermally annealing even without the covering of the second Ti film on top. It is noticed from the recorded AFM images that some Ti grains are visible on top of the nanotube surface, which indicates the migration of the Ti grains during thermal annealing and the good wettability of Ti on CNT surfaces. There is no sign that thermal annealing leads to any structural degradation of nanotubes, or the thermal-induced Ti grain migration results in any substantial lateral bending of nanotubes. The AFM measurements also reveal that the thermal annealing results in a 26% increase of the Ti grain size from about 26 nm to about 34 nm.

Fig. 1(c) shows the fractured surface of a thermally annealed CNT–Ti composite specimen with a number of sparsely distributed thin and long protruding structures. The protruding structures were characterized by using transmission electron microscopy inside a JEM 2100F TEM (JEOL Ltd.), which is exemplified by the image in Fig. 1(d), and were confirmed as individual

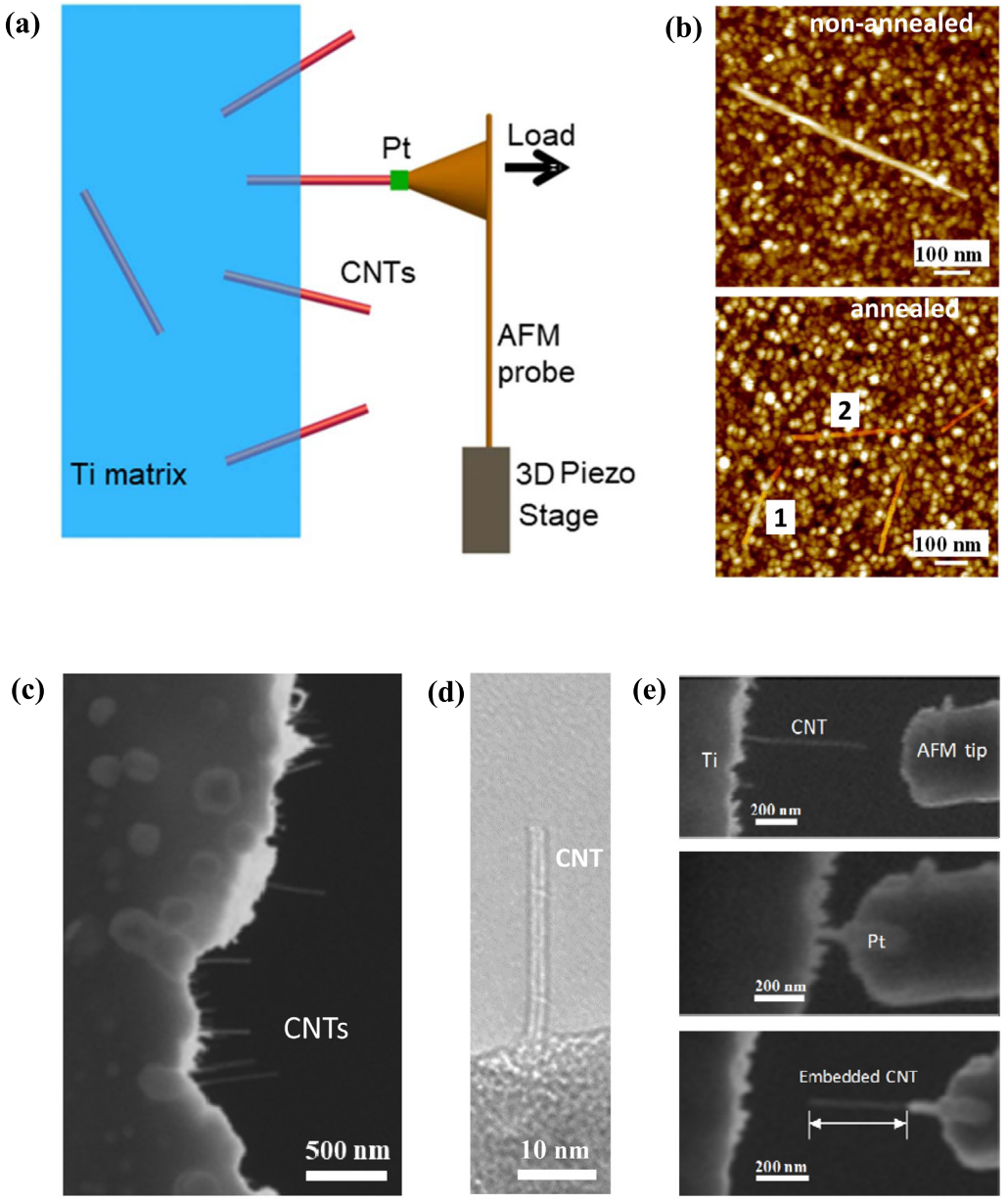

Fig. 1. Nanomechanical characterization of the interfacial strength of thermally annealed CNT–Ti nanocomposites. (**a**) Schematic of an *in situ* SEM nanomechanical single-nanotube pull-out testing technique based on nanomanipulation using a high-resolution 3D piezo actuator stage. (**b**) AFM images of deposited CNTs on the surfaces of electron beam deposited Ti metal films: (top) before thermal annealing (the nanotube has a length of 600 nm and a diameter of 4.0 nm); (bottom) after thermal annealing (fake red color is added to aid visualization): Ti metal grains are visible on top of the surface of the marked nanotubes #1 and #2. (**c**) One of the selected specimens that were employed in the nanomechanical measurements. (**d**) TEM image of one protruding nanotube (about 2.9 nm in outer diameter). (**e**) Selected SEM snapshots showing the processes of mechanically pulling out one free-standing nanotube using an AFM cantilever with the aid of the electron beam induced deposition of Pt. The bottom image shows the embedded portion of the tested nanotube after it was completely pulled out of the metal matrix. (For interpretation of the references to color in this figure legend, the reader is referred to the web version of this article.)

tubular nanostructures with diameters that are consistent with the employed DWCNTs.

(c) *In situ SEM single-nanotube pull-out measurements* Fig. 1(e) shows selected SEM snapshots of one single-nanotube pull-out experiment that was conducted on a thermally annealed CNT–Ti nanocomposite specimen. In brief, an AFM probe tip was controlled to approach and contact the free end of one selected CNT that was oriented along the tip axis direction (i.e., the AFM stretching force direction). The free end of the CNT was subsequently welded to the AFM probe tip by using electron beam induced deposition (EBID) of Pt for a firm attachment. A gradually increasing stretching force was applied to the CNT by the AFM cantilever till the embedded portion of the nanotube was stretched out of the matrix, as shown in the bottom image in Fig. 1(e). For this single-nanotube pull-out measurement, the applied pull-out force and the embedded nanotube length were measured to be about 74 nN and about 393 nm, respectively. In addition to the successful single-nanotube pull-out events as shown in Fig. 1(e), our *in situ* nanomechanical experiments also captured two other types of failure scenarios: fracture of the protruding nanotube segment and telescopic pull-out. The former failure scenario, which is exhibited by the SEM snapshots in Figure S1(a), occurs when the stretching force exceeds the fracture strength of the nanotube and fractures the nanotube at its protruding segment. The latter failure scenario, as exemplified by the SEM snapshots displayed in Figure S1(b), occurs when

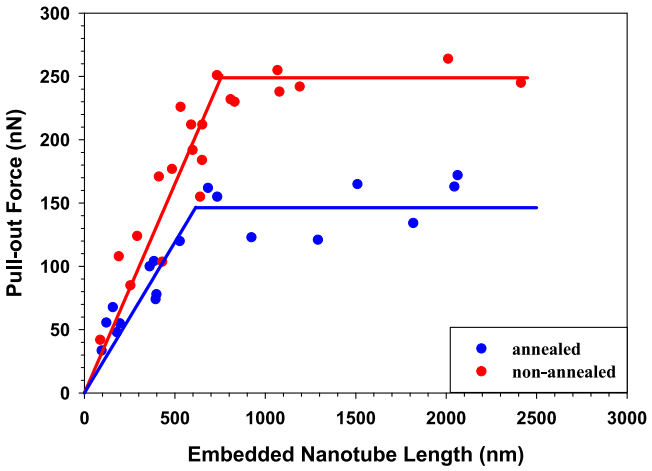

Fig. 2. The measured dependence of the pull-out force on the embedded nanotube length for thermally annealed (blue dots) and non-annealed (red dots, reproduced from Ref. [10]) CNT–Ti interfaces. The solid lines are the bilinear fitting curves. (For interpretation of the references to color in this figure legend, the reader is referred to the web version of this article.)

the stretching force breaks the outmost shell(s) of the protruding nanotube and pulls out the inner tube shell(s). Both types of failure scenarios represent the mechanical failure of the nanotube, instead of the nanotube–metal interface, and are therefore excluded in the further analysis of the interfacial load transfer characteristics of the nanotube–metal interface. We want to highlight that the byproduct of the pullout experiments, i.e. AFM probe with an attached nanotube tip, can be used as ultrasharp machining tools to manufacture ultrafine patterns.

We have conducted a number of single-nanotube pull-out experiments on thermally annealed sandwiched CNT–Ti composite specimens using the testing scheme illustrated in Fig. 1(a). The blue dots in Fig. 2 show the measured pull-out force as a function of the embedded nanotube length based on 18 different experiments that led to actual nanotube pull-out from the thermally annealed CNT–Ti composites. Two distinct trends are exhibited in the measurement data that are fitted using a bilinear dash-line curve. The pull-out force is found to first increase in a nearly linear trend with the embedded nanotube length and then form a plateau with a narrow force fluctuation range, which is calculated to be 146 ± 21 nN. The displayed bilinear trend in the pull-out force measurement is a clear indication that the interfacial load transfer on the thermally annealed CNT–Ti interface follows the so called "shear-lag" effect and the nanotube pull-out is an energy-driven interfacial debonding phenomenon as a result of crack initiation and propagation on the nanotube–metal interface [9,10].

For the purpose of comparison, Fig. 2 also displays the measured pull-out force data from a prior nanomechanical study on the interfacial strength of CNT–Ti composite specimens that were prepared and tested by using the same batches of nanotube and metal materials and by following the same experimental protocols as the present study except that the tested composite specimens were not subjected to any thermal annealing treatments. The pull-out measurement data that were obtained on the non-annealed composite specimens follow a similar trend with those on thermally annealed specimens, but possess a steeper slope in the initial linearly increasing segment and a much higher force value at its plateau that is reported to be ~245 nN [10]. The comparison displayed in Fig. 2 indicates that the CNT–Ti interface is substantially weakened by the thermal annealing process and its maximum interfacial load-carrying capacity that is measured as the force level of the plateau is reduced by about 40%, even though the overall shear-lag type interfacial load transfer characteristics remain unaltered. It is plausible that the weaker interface from thermal annealing could be one of the factors that lead to the observed bulk property degradation in thermally treated CNT–Ti MMNC [18]. It is noted that the relatively larger data scattering exhibited in the measured pull-out force values for annealed specimens is a possible indicator that thermal annealing might have caused some degree of non-uniformities on the CNT–Ti interface.

To the best of our knowledge, this study reports the first direct and quantitative experimental findings that thermal processing substantially weakens the interfacial strength of CNT–Ti composites. The nanomechanical measurements demonstrate that the *in situ* single-nanotube pull-out technique is capable of revealing the influence of thermal processing on the mechanical signature of the CNT–metal interface. The results suggest that it is plausible that facile thermal processing can be utilized to effectively control the bulk mechanical properties of CNT–Ti nanocomposites through tuning their interfacial strength. The findings will be helpful to understand the impact of thermal processing on the reinforcing mechanism of nanotubes in metal matrices and to the optimal design and manufacturing of nanotube-reinforced MMNC for superior performance and functionality. It is worth mentioning that the presented *in situ* single-nanotube pull-out experiments may not be directly applicable to conventionally manufactured bulk nanotube–metal composites, which usually possess much more irregular configurations of nanotube–metal interfaces as compared to the model specimens used in our study.

2.2. Theoretical predictions of the interfacial shear stress distribution profile on mechanically loaded CNT–Ti interfaces

We investigate the interfacial load transfer characteristics of the thermally annealed CNT–Ti interface by using a micromechanics shear-lag model. As illustrated in the single-nanotube nanocomposite configuration shown in Fig. 3(a), a CNT with a diameter D_{nt} is partially embedded into a concentric cylindrical metal matrix with an embedded length L and a uniform interfacial contact. The interfacial shear stress (IFSS), τ, is developed to balance the stretching force applied to the protruding end of the nanotube P, which is given as $\pi D_{nt} \int_0^L \tau(z)dz = P$, where z is the coordinate along the nanotube's longitudinal axis ($z = 0$ at the embedded end). The point-wise IFSS on the nanotube–metal interface possesses its maximum value at the nanotube entry position (i.e., $z = L$), where the interface failure initiates. The nanotube is considered a linearly elastic material with a Young's modulus E_{nt}, while the metal matrix is modeled as a linearly elastic and perfectly plastic material with a Young's modulus E_m, a Poisson's ratio ν_m and a yield shear stress τ_Y. For simplicity, the metal matrix deformation that is caused by the interfacial shear force is assumed to occur only in a thin interfacial matrix layer that is in direct binding contact with the nanotube surface. The interfacial matrix layer undergoes pure shear deformation, which can be generally divided into two zones: (1) unsaturated zone, where the deformation is purely elastic. (2) saturated zone, where the IFSS is capped by a certain value. The observed clean nanotube pull-out (Fig. 1(d)) indicates no matrix failure. Therefore, the IFSS should not exceed the yield shear stress of the matrix material. Therefore, the IFSS is either capped by the yield shear stress of the matrix material τ_Y or is capped by a value τ^* that is governed by the interfacial binding interaction and is lower than the yield shear stress of the matrix material.

The equilibrium of the nanotube along its longitudinal direction is given as

$$\sigma_z \cdot D_{nt} - 4\int_0^z \tau dz = 0, \tag{1}$$

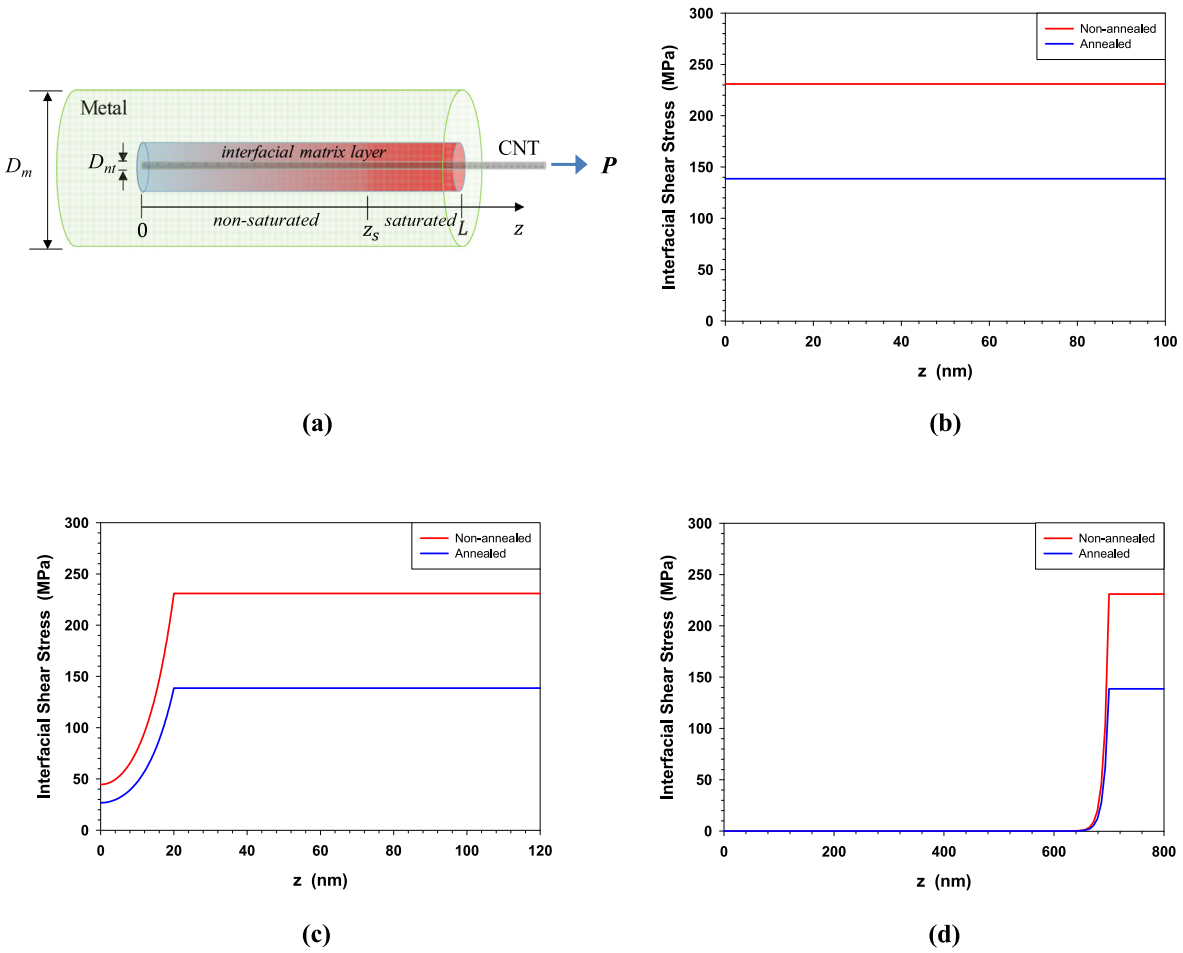

Fig. 3. (a) Schematic of the micromechanics model of single nanotube–metal composite that is commensurable to the single-nanotube pull-out measurement. The diameter of the metal cylinder D_m is about 200 nm. (b)–(d) Representative theoretically predicted interfacial shear stress distribution profiles on non-annealed (red curves) and thermally-annealed (blue curves) CNT–Ti interfaces with an assumed nanotube length of 100 nm (b), 120 nm (c) and 800 nm (d). (For interpretation of the references to color in this figure legend, the reader is referred to the web version of this article.)

The entire interfacial matrix layer comprises either a fully unsaturated zone, mixed unsaturated and saturated zones, or a fully saturated zone. For the general case of mixed unsaturated and saturated zones, in the unsaturated zone ($0 \le z < z_s$, where z_s indicates the position where the IFSS starts to saturate), τ is given as $\tau(z) = \frac{E_m}{2(1+\nu_m)} \cdot \frac{u(z)}{t}$, in which $u(z)$ is the nanotube displacement, and t is the thickness of the interfacial matrix layer and is the only fitting parameter in the model. By considering the normal stress in the nanotube that is given by $\sigma_z = E_{nt}\frac{du(z)}{dz}$. In the saturated zone ($z_s \le z \le L$), $\tau(z) = \tau_Y$ or τ^*. By inserting these relationships into Eq. (1), we get

$$D_{nt}\frac{d^2u(z)}{dz^2} - \frac{2E_m}{t(1+\nu_m)}\sigma(z) = 0, \qquad 0 \le z < z_s \tag{2a}$$

$$D_{nt}\cdot E_{nt}\frac{d^2u(z)}{dz^2} - 4\tau_Y(or\,\tau^*) = 0. \qquad z_s \le z \le L \tag{2b}$$

The boundary conditions are $\sigma_z = 0$ at $z = 0$ and $u(z) = \frac{2(1+\nu_m)\cdot t\cdot\tau_Y}{E_m}$ at $z = z_s$.

We analyze the IFSS distribution on CNT–Ti interfaces using the above micromechanics model based on the nanomechanical single-nanotube pull-out measurement data shown in Fig. 2. Fig. 3(b)–(d) show representative IFSS distribution profiles that are calculated based on three selected embedded nanotube lengths of 100 nm, 120 nm, and 800 nm, respectively. The following parameters are employed in the calculations: $E_{nt} = 1.0$ TPa and $D_{nt} = 3.1$ nm for CNTs, $E_m = 116$ GPa, $\nu_m = 0.32$, $\tau_Y = 231$ MPa for Ti [10], and $t = 5.3$ nm. For $L = 800$ nm, the applied pull-out force is the measured average plateau force value (i.e., $P = 245(146)$ nN (non-annealed (annealed)). The respective pull-out forces for $L = 100$ nm and $L = 120$ nm are calculated based on the same maximum IFSS that is found for $L = 800$ nm and are found to be 225 (134) nN and 244 (146) nN, respectively. Our IFSS analysis of non-annealed CNT–Ti interfaces, as shown by the red plots in Fig. 3(b)–(d), reveals that the entire interfacial matrix layer yields upon the nanotube pull-out for $L = 100$ nm. Matrix yielding is also observed for longer embedded lengths $L = 120$ nm and $L = 800$ nm, whose curves also include the unsaturated (elastic) zone. The analysis shows that the maximum IFSS of non-annealed CNT–Ti interface is limited by the yield shear stress of the metal matrix. The IFSS distribution profiles for the corresponding thermally annealed interfaces, which are exhibited as blue plots in Fig. 3(b)–(d), follow a similar trend with those of the comparable non-annealed interfaces, but possess a much lower capped value (135 MPa) that is about 42% below the yield shear stress of Ti materials (non-annealed). The lower IFSS value for the annealed CNT–Ti interface is attributed to the weaker interfacial binding interactions from reactions products caused by thermal annealing [7,17]. In addition, the possible lower yield stress of Ti materials after thermal annealing, which reportedly corresponds to the observed thermal-induced metal grain size increase [19,20], may contribute to the observed interface weakening. The interfacial stress analysis here does not take

into account any influence of the residual stress that may occur during the sample preparation and annealing processes.

2.3. Characterization of thermal oxidation on thermally annealed CNT–Ti interfaces

The observed substantial thermal-induced interface weakening can be attributed to multiple sources related to the thermal reaction products formed on the CNT–Ti interface [13,14,25,26] as well as the microstructure and mechanical changes of the Ti matrix structures caused by thermal annealing [16,19,20]. Even though the Ti film deposition was conducted in high vacuum environments, a thin layer of titanium oxide inevitably formed on its surface once in contact with oxygen and water vapor in air or water in the deposited CNT solutions, as illustrated in Fig. 4(a). The thermal annealing likely leads to newly grown oxide on the metal surfaces and the CNT–metal interface, which is illustrated in Fig. 4(b). The existence of oxygen reportedly weakens the CNT–Ti binding interaction because Ti atoms preferably bind to the surrounding oxygen atoms as compared to carbon atoms [26]. Ti can also form titanium carbide (TiC) through reaction with carbon atoms. However, it is unlikely that TiC exists on the tested CNT–Ti interface because the thermal annealing temperature in the present study (400 °C) is well below the reported formation temperature for TiC (700–800 °C) [27,28]. Here we conducted detailed surface analysis measurements by using X-ray photoelectron spectroscopy (XPS), ellipsometry, and AFM to characterize and quantify the growth of titanium oxide in the thermally annealed CNT–Ti nanocomposites specimen. The XPS measurements were conducted using a PHI 5000 VersaProbe instrument (Physical Electronics, Inc.), which employs monochromatic Al K_α X-rays of energy 1486.6 eV. Ellipsometry characterization was performed using a UVISEL spectroscopic ellipsometer (Horiba) in the 1.5 eV to 6.5 eV spectral range.

XPS measurements of freshly electron beam evaporated single-layer Ti films (∼100 nm in thickness) at room temperature, which are displayed in Fig. 4(c), show a thin native oxide layer on the surface of pure Ti, which is represented by the peaks at 458.4 eV and 464 eV. The sampling depth of the XPS measurement is ∼5 nm on average, so the presence of a peak at 453.8 eV, which corresponds to metallic Ti, indicates that the thickness of the oxide layer is less than 5 nm [29]. The absence of the metallic peak after two hours annealing of the specimen at 400 °C in air confirms the presence of a much thicker oxide layer. To quantify the thickness of the oxide layer, argon ion sputter etching was performed to obtain XPS depth profiling data, which are shown in Figure S2. Ar^+ sputtering was performed at 1 kV, which was calibrated to give a SiO_2 etch rate of 3.3 nm/min. Spectra of Ti(2p) and O(1s) were acquired every minute with an etch rate of ∼1.89 nm/min for TiO_2, which sputters ∼0.57 times slower than SiO_2. Before etching of the oxide film, the $Ti2p_{1/2}$ (464 eV) and $Ti2p_{3/2}$ (458.4 eV) peaks were observed, which can be identified as peaks that correspond to TiO_2. After five etching cycles, the metallic Ti peak (453.8 eV) reappears, and the Ti(2p) and O(1s) profiles intersect at ∼6.5 min sputtering time which gives the thickness of the oxide layer in the annealed specimen to be ∼12.3 nm. The XPS measurement data are consistent with ellipsometry measurements that show a ∼5 nm oxide layer formed on a single-layer Ti film surface after the deposition of CNT solutions. The thickness of the oxide layer was found to grow to 9.9 nm, 11.1 nm, and 12.5 nm after 30 min, 1 h, and 2 h thermal annealing at 400 °C in air, respectively. The ellipsometry measurements indicate the growth rate of the oxide layer slows down during thermal annealing, which can be attributed to the role of the passivation barrier by the existing oxide layer.

Fig. 4(d) shows the AFM topographic line-scanning measurements that were performed on a single-layer (∼100 nm in thickness) Ti film and a sandwiched Ti/CNT/Ti composite film (∼200 nm in thickness) before and after two-hour thermal annealing at 400 °C in air. A piece of copper tape was placed over the Si substrate prior to metal deposition to provide a flat reference surface for AFM scanning. The thickness (height) of the single-layer film is found to increase by ∼7.2 nm from 103.7 nm to 110.9 nm after thermal annealing, which is attributed to the growth of the oxide layer on the metal top surface. The height of the sandwiched composite film is found to increase by ∼9.9 nm from 209.4 nm to 219.3 nm. The measurements indicate that there is an additional expansion by about ∼2.7 nm inside the sandwiched composite film in addition to the oxide growth on the top metal surface, which is assumed to be the same for both samples. The observed expansion is attributed to the newly grown oxide on the CNT–Ti interfaces through thermal oxidation during the thermal annealing process. The substantially slow oxide growth around the nanotube–metal interface region as compared to those occurring on the metal top surface that is completely exposed to air indicates a much lower local oxygen concentration around the interface region. The possible sources of oxygen for the thermal oxidation on the CNT–metal interface include the oxygen molecules that are diffused through the metal film surface and spacings between metal grains and nanotube surfaces, and/or transported through the hollow shells of those open-ended nanotubes [30].

3. Conclusions

The impact of thermal processing on the interfacial strength of CNT reinforced Ti nanocomposites was quantitatively investigated by using an *in situ* SEM nanomechanical characterization technique. The nanomechanical measurements reveal that thermal annealing substantially weakens the CNT–Ti interface, which is ascribed to the thermal oxidation of metal grains that are in direct contacts with nanotube surfaces. The observed thermal-induced interfacial weakening in CNT–Ti composite is contrasted with previously reported substantial interfacial strengthening in thermally annealed CNT-Al composites, which indicates the sophisticated role of oxidation in the interfacial load transfer and the resulting bulk mechanical properties of CNT-reinforced MMNC. The findings reported here are useful to better understand the impact of thermal processing on the reinforcing efficiency of nanotubes in metal matrices, which is essential to the design and manufacturing of nanotube-reinforced MMNC with superior high-temperature performance.

Declaration of competing interest

The authors declare that they have no known competing financial interests or personal relationships that could have appeared to influence the work reported in this paper.

Acknowledgments

This work was supported by the United States Air Force Office of Scientific Research — Low Density Materials program under Grant No. FA9550-15-1-0491, and by the National Science Foundation under Grant Nos. CMMI-1537333, CMMI-2006127 and CMMI-2009134. We thank Dr. In-Tae Bae for his assistance with the TEM characterization. C.M.D acknowledges fellowship support from the New York NASA Space Grant Consortium.

Appendix A. Supplementary data

Supplementary material related to this article can be found online at https://doi.org/10.1016/j.eml.2020.101045.

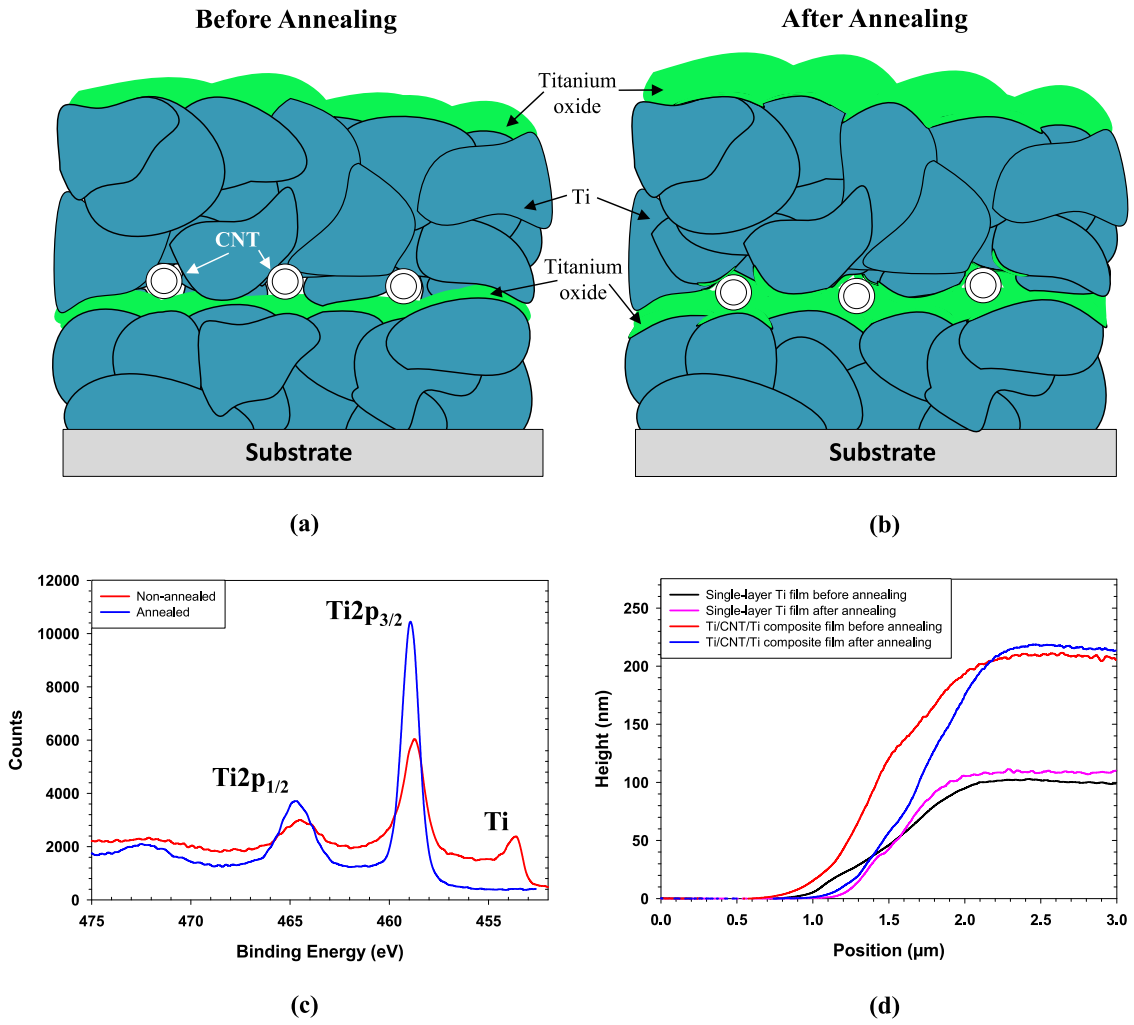

Fig. 4. Characterization of thermal oxidation in CNT–Ti composites. (a–b) Schematic drawings about the evolution of the oxidation inside the CNT–Ti nanocomposites before (a) and after (b) thermal annealing. (c) Ti(2p) XPS measurements of the freshly deposited Ti film before (red curve) and after (blue curve) thermal annealing. (d) Comparison of the AFM height (thickness) measurements on the deposited single-layer Ti films and the sandwiched Ti/CNT/Ti composite films before and after thermally annealing. (For interpretation of the references to color in this figure legend, the reader is referred to the web version of this article.)

References

[1] S.R. Bakshi, D. Lahiri, A. Agarwal, Carbon nanotube reinforced metal matrix composites - a review, Int. Mater. Rev. 55 (2013) 41, http://dx.doi.org/10.1179/095066009X12572530170543.

[2] S.P. Rawal, Metal-matrix composites for space applications, JOM 53 (2001) 14–17, http://dx.doi.org/10.1007/s11837-001-0139-z.

[3] F. Banhart, Interactions between metals and carbon nanotubes : at the interface between old and new materials, Nanoscale 1 (2009) 201–213, http://dx.doi.org/10.1039/B9NR00127A.

[4] A. Naseer, F. Ahmad, M. Aslam, B.H. Guan, W.S.W. Harun, N. Muhamad, M.R. Raza, R.M. German, A review of processing techniques for graphene-reinforced metal matrix composites, Mater. Manuf. Process. 34 (2019) 957–985, http://dx.doi.org/10.1080/10426914.2019.1615080.

[5] C.A. Isaza Merino, J.E. Ledezma Sillas, J.M. Meza, J.M. Herrera Ramirez, Metal matrix composites reinforced with carbon nanotubes by an alternative technique, J. Alloys Compd. 707 (2017) 257–263, http://dx.doi.org/10.1016/j.jallcom.2016.11.348.

[6] M. Antillon, P. Nautiyal, A. Loganathan, B. Boesl, A. Agarwal, Strengthening in boron nitride nanotube reinforced aluminum composites prepared by roll bonding, Adv. Energy Mater. 20 (2018) 1800122, http://dx.doi.org/10.1002/adem.201800122.

[7] S. Bagchi, C. Ke, H.B. Chew, Oxidation effect on the shear strength of graphene on aluminum and titanium surfaces, Phys. Rev. B 98 (2018) 174106, http://dx.doi.org/10.1103/PhysRevB.98.174106.

[8] R. George, K.T. Kashyap, R. Rahul, S. Yamdagni, Strengthening in carbon nanotube/aluminium (CNT/Al) composites, Scr. Mater. 53 (2005) 1159–1163, http://dx.doi.org/10.1016/j.scriptamat.2005.07.022.

[9] C. Yi, X. Chen, F. Gou, C.M. Dmuchowski, A. Sharma, C. Park, C. Ke, Direct measurements of the mechanical strength of carbon nanotube - Aluminum interfaces, Carbon 125 (2017) 93–102, http://dx.doi.org/10.1016/j.carbon.2017.09.020.

[10] C. Yi, S. Bagchi, C.M. Dmuchowski, F. Gou, X. Chen, C. Park, H.B. Chew, C. Ke, Direct nanomechanical characterization of carbon nanotubes - titanium interfaces, Carbon 132 (2018) 548–555, http://dx.doi.org/10.1016/j.carbon.2018.02.069.

[11] T. Kuzumaki, O. Ujiie, H. Ichinose, K. Ito, Mechanical characteristics and preparation of carbon nanotube fiber-reinforced Ti composite, Adv. Energy Mater. 2 (2000) 416–418, http://dx.doi.org/10.1002/1527-2648(200007)2:7<416::AID-ADEM416>3.0.CO;2-Y.

[12] C. Leyens, M. Peters, Titanium and Titanium Alloys: Fundamentals and Applications, John Wiley & Sons, 2003.

[13] K. Kondoh, T. Threrujirapapong, H. Imai, J. Umeda, B. Fugetsu, Characteristics of powder metallurgy pure titanium matrix composite reinforced with multi-wall carbon nanotubes, Compos. Sci. Technol. 69 (2009) 1077–1081, http://dx.doi.org/10.1016/j.compscitech.2009.01.026.

[14] F.-C. Wang, Z.-H. Zhang, Y.-J. Sun, Y. Liu, Z.-Y. Hu, H. Wang, A.V. Korznikov, E. Korznikova, Z.-F. Liu, S. Osamu, Rapid and low temperature spark plasma sintering synthesis of novel carbon nanotube reinforced titanium matrix composites, Carbon 95 (2015) 396–407, http://dx.doi.org/10.1016/j.carbon.2015.08.061.

[15] S. Li, B. Sun, H. Imai, T. Mimoto, K. Kondoh, Powder metallurgy titanium metal matrix composites reinforced with carbon nanotubes and graphite, Composites A 48 (2013) 57–66, http://dx.doi.org/10.1016/j.compositesa.2012.12.005.

[16] K.S. Munir, Y. Zheng, D. Zhang, J. Lin, Y. Li, C. Wen, Microstructure and mechanical properties of carbon nanotubes reinforced titanium matrix

composites fabricated via spark plasma sintering, Mater. Sci. Eng. A 688 (2017) 505–523, http://dx.doi.org/10.1016/j.msea.2017.02.019.
[17] Y. Matsuda, W.-Q. Deng, W.A. Goddard, Contact resistance properties between nanotubes and various metals from quantum mechanics, J. Phys. Chem. C 111 (2007) 11113–11116, http://dx.doi.org/10.1021/jp072794a.
[18] K. Kondoh, T. Threrujirapapong, J. Umeda, B. Fugetsu, High-temperature properties of extruded titanium composites fabricated from carbon nanotubes coated titanium powder by spark plasma sintering and hot extrusion, Compos. Sci. Technol. 72 (2012) 1291–1297, http://dx.doi.org/10.1016/j.compscitech.2012.05.002.
[19] Z. Li, L. Fu, B. Fu, A. Shan, Effects of annealing on microstructure and mechanical properties of nano-grained titanium produced by combination of asymmetric and symmetric rolling, Mater. Sci. Eng. A 558 (2012) 309–318, http://dx.doi.org/10.1016/j.msea.2012.08.005.
[20] A.V. Polyakov, I.P. Semenova, E.V. Bobruk, S.M. Baek, H.S. Kim, R.Z. Valiev, Impact toughness of ultrafine-grained commercially pure titanium for medical application, Adv. Energy Mater. 20 (2018) 1700863, http://dx.doi.org/10.1002/adem.201700863.
[21] X. Chen, L. Zhang, M. Zheng, C. Park, X. Wang, C. Ke, Quantitative nanomechanical characterization of the van der Waals interfaces between carbon nanotubes and epoxy, Carbon 82 (2015) 214–228, http://dx.doi.org/10.1016/j.carbon.2014.10.065.
[22] X. Chen, L. Zhang, C. Park, C.C. Fay, X. Wang, C. Ke, Mechanical strength of boron nitride nanotube-polymer interfaces, Appl. Phys. Lett. 107 (2015) 253105, http://dx.doi.org/10.1063/1.4936755.
[23] X. Chen, M. Zheng, C. Park, C. Ke, Direct measurements of the mechanical strength of carbon nanotube–poly(methyl methacrylate) interfaces, Small 9 (2013) 3345–3351, http://dx.doi.org/10.1002/smll.201202771.
[24] C. Yi, S. Bagchi, F. Gou, C.M. Dmuchowski, C. Park, C.C. Fay, H.B. Chew, C. Ke, Direct nanomechanical measurements of boron nitride nanotube—ceramic interfaces, Nanotechnology 30 (2019) 025706, http://dx.doi.org/10.1088/1361-6528/aae874.
[25] T. Taguchi, H. Yamamoto, S. Shamoto, Synthesis and characterization of single-phase TiC nanotubes, TiC nanowires, and carbon nanotubes equipped with TiC nanoparticles, J. Phys. Chem. C 111 (2007) 18888–18891, http://dx.doi.org/10.1021/jp0756909.
[26] A. Felten, I. Suarez-Martinez, X. Ke, G. Van Tendeloo, J. Ghijsen, J.-J. Pireaux, W. Drube, C. Bittencourt, C.P. Ewels, The role of oxygen at the interface between titanium and carbon nanotubes, ChemPhysChem 10 (2009) 1799–1804, http://dx.doi.org/10.1002/cphc.200900193.
[27] R. Martel, T. Schmidt, H.R. Shea, T. Hertel, P. Avouris, Single- and multi-wall carbon nanotube field-effect transistors, Appl. Phys. Lett. 73 (1998) 2447–2449, http://dx.doi.org/10.1063/1.122477.
[28] F. Xue, S. Jiehe, F. Yan, C. Wei, Preparation and elevated temperature compressive properties of multi-walled carbon nanotube reinforced Ti composites, Mater. Sci. Eng. A 527 (2010) 1586–1589, http://dx.doi.org/10.1016/j.msea.2009.12.003.
[29] A. Felten, I. Suarez-Martinez, X. Ke, G. Van Tendeloo, J. Ghijsen, J.-J. Pireaux, W. Drube, C. Bittencourt, C.P. Ewels, The role of oxygen at the interface between titanium and carbon nanotubes, ChemPhysChem 10 (2009) 1799–1804, http://dx.doi.org/10.1002/cphc.200900193.
[30] K.-H. Lee, S.B. Sinnott, Equilibrium and nonequilibrium transport of oxygen in carbon nanotubes, Nano Lett. 5 (2005) 793–798, http://dx.doi.org/10.1021/nl0502219.